Monatshefte für Chemie 128, 1–12 (1997)

Monatshefte für Chemie
Chemical Monthly

Studies of the Mixed Adsorption Layer on a Mercury Electrode in the System *p*-Toluidine-Polyethyleneglycol-1 *M* $NaClO_4$

J. Saba

Faculty of Chemistry, M. Curie-Skłodowska University, PL-20031 Lublin, Poland

Summary. The properties of the mixed adsorption layer on a mercury electrode in the system 1 *M* $NaClO_4$-*p*-toluidine-polyethyleneglycol (average molecular masses of polyethyleneglycols: 400 or 10000) are discussed. The parameters of the *Frumkin* and virial isotherms were determined in the range of strong adsorption potentials. In the range of more negative potentials, a mixed adsorption layer was found by investigating the kinetics of the reduction of Zn(II) ion as a pilot ion. Depending on the concentration ratio of the studied organic substances, inhibition, acceleration, or compensation of both with respect to Zn(II) electroreduction was observed. In the presence of polyethyleneglycol, the efficiency of the Zn(II) ion electroreduction increases due to a greater adsorption lability of *p*-toluidine molecules on the mercury surface.

Keywords. Mixed adsorption layer; Equilibrium of adsorption; Reduction of Zn(II) ion; Adsorption isotherms.

Untersuchung der gemischten Adsorptionsschicht an einer Quecksilberelektrode im System *p*-Toluidin-Polyethyleneglycol-1 *M* $NaClO_4$

Zusammenfassung. Die Eigenschaften der gemischten Adsorptionsschicht an einer Quecksilberelektrode im System 1 *M* $NaClO_4$-*p*-Toluidin-Polyethyleneglycol (durchschnittliche Molmassen der Polyethylenglycole: 400 bzw. 1000) werden diskutiert. Die Parameter der *Frumkin*- und Virialisotherme wurden im Bereich hoher Adsorptionspotentiale bestimmt. Im Bereich negativerer Potentiale wurde durch Untersuchung der Kinetik der Elektroreduktion von Zn(II)-Ionen als Pilotionen eine gemischte Adsorptionsschicht gefunden. In Abhängigkeit von der Konzentration der organischen Verbindungen beobachtet man bezüglich der Elektroreduktion von Zn(II) Hemmung, Beschleunigung oder eine gegenseitige Kompensation beider Effekte. In Gegenwart von Polyethyleneglycol nimmt die Effizienz der Elektroreduktion von Zn(II) aufgrund einer höheren Adsorptionslabilität der *p*-Toluidin-Moleküle an der Quecksilberoberfläche zu.

Introduction

Adsorption studies of organic substances on a mercury electrode enable closer insight into the electrical structure of the double layer [1, 2] and its effect on the

electrode processes [3]. Earlier studies on the acceleration of the electroreduction of Zn(II) ions by some organic substances [4, 5] have allowed to choose pairs of organic substances causing inhibiting and accelerating effects on the above mentioned reduction process, respectively.

Among such pairs of organic substances there should be mentioned: *n*-butanol and thiourea [6], *n*-butanol and toluidine [7], polyethyleneglycol and thiourea [8]. The values of standard rate constants of Zn(II) reduction indicate that inhibition, acceleration, and compensation depend on the concentrations of these substances. That confirms the existence of a mixed adsorption layer in the range of the Zn(II) ion reduction potential. Studies of the coadsorption of the above mentioned substances on a mercury electrode show the congruency of the obtained isotherms versus the electrode charge. The decrease in the free energy of adsorption $\Delta\bar{G}^0$ for thiourea and toluidine in the presence of the given inhibitor is also observed. In turn, the interaction constant values obtained from the *Frumkin* and virial isotherms indicate that the orientation of the thiourea molecules changes depending on the electrode charge in the presence of both *n*-butanol and polyethyleneglycols. However, the orientation of toluidine molecules in the presence of *n*-butanol remains unchanged. It has also been stated that the adsorption of toluidine in the presence of the studied inhibitors is stronger compared with thiourea [9].

This paper presents the results of studies on the coadsorption of *p*-toluidine (*pT*) and polyethyleneglycols of an average molecular mass of 400 (*PEG 400*) or 10000 (*PEG 10000*). Adsorption of *pT* in the range of potentials close to that of zero charge (*pzc*) for 1 *M* $NaClO_4$ and in the presence of a selected *PEG* was characterized by means of the parameters of the *Frumkin* and virial isotherms. In the range of potentials more distant from *pzc*, kinetic studies of the reduction of Zn(II) ion as a pilot ion were applied to determine properties of the mixed adsorption layer of *pT-PEG 400* or *pT-PEG 10000*.

Results and Discussion

Analysis of experimental data

A differential capacity decrease with the addition of *PEG 400* or *PEG 10000*, characteristic for typical inhibitors, is observed. The potential range in which the decrease takes place reaches from -0.35 V to -1.60 V for $5 \cdot 10^{-4}$ *M PEG*; it is still larger for *PEG 10000*. The differential capacity decrease is larger for *PEG 10000* than for *PEG 400* and is practically independent of its concentration. Both size and shape of the molecules of *PEG* under consideration influence the effect. According to *Rösch* [10, 11], *PEG* molecules of mer number $n < 11$ (unit of repetition: $-CH_2-O-CH_2-$) possess a zig-zag structure; when $n > 11$, a meander structure is found.

In the differential capacity curves obtained in 1 *M* $NaClO_4$, a well formed desorption peak is observed upon addition of *pT*. Its potential shifts from -1.02 V to -1.32 V when the *pT* concentration increases. The adsorption peak is only slightly marked.

Figures 1 and 2 present the differential capacity curves of 10^{-4} *M PEG 400* or *PEG 10000* solutions with increasing amount of *pT*. The course of these curves is quite different compared with the curves for the solutions containing only *PEG* or

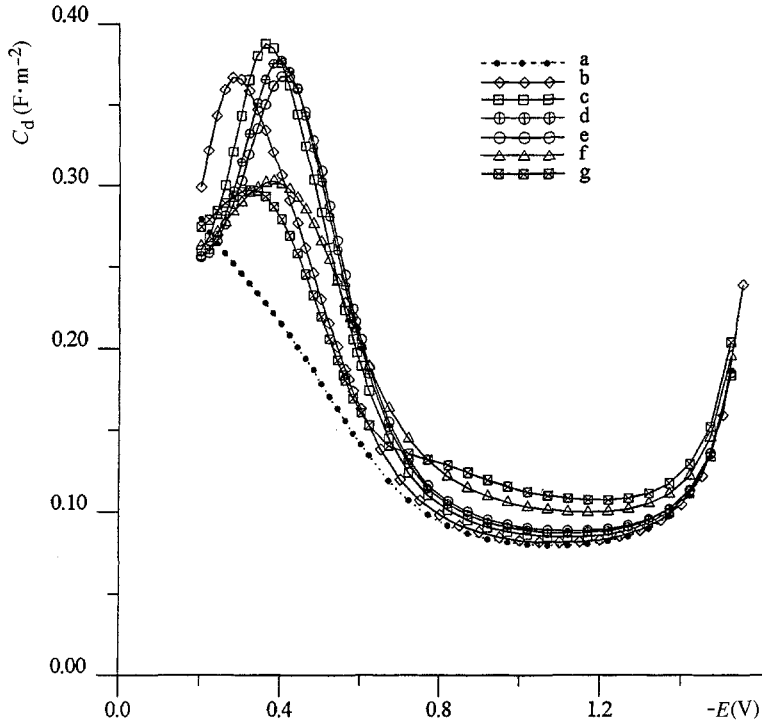

Fig. 1. Differential capacity curves of Hg/1 *M* $NaClO_4 + 10^{-4}$ *M PEG 400* for different contents of *pT*; a) 0 *M*, b) 0.0015 *M*, c) 0.005 *M*, d) 0.008 *M*, e) 0.01 *M*, f) 0.03 *M*, g) 0.05 *M*

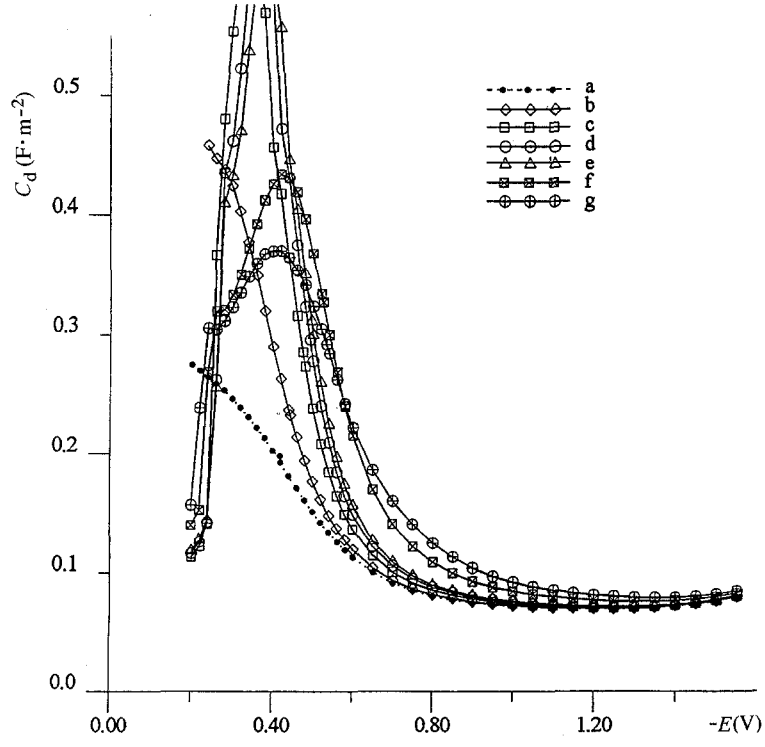

Fig. 2. Differential capacity curves of Hg/1 *M* $NaClO_4 + 10^{-4}$ *M PEG 10000* for different contents of *pT* as indicated in Fig. 1

only *pT*: there is a lack of *pT* desorption peaks. However, in the potential range from −0.2 V to −0.6 V, well formed adsorption peaks are observed which are much more intense in the presence of *PEG 10000* than in that of *PEG 400*. They may be caused by the competitive character of the adsorption of *pT* and *PEG* molecules rather than by the change of the orientation of *pT* molecules as postulated earlier [12]. It should be emphasized that the addition of *pT* to a solution containing *PEG 400* causes a differential capacity increase over the whole potential range studied; for *PEG 10000*, this situation takes place only for $c_{pT} > 0.01\ M$.

The capacity *vs.* the potential data curve was numerically integrated from the point of *pzc*. The integration constants are presented in Fig. 3 and Table 1. As follows from Fig. 3, the *pzc* values shift towards positive potentials is the solutions containing only *PEG*. This fact confirms the orientation of *PEG* molecules on the mercury surface as postulated by *Jehring* [13]: the $-CH_2-O-CH_2-$ group oxygen is oriented towards the solution, whereas the carbon atoms – being the positive moiety of the dipole – adsorb on the mercury. At low *pT* concentrations, the π-system of *pT* lies flat on the metal surface [14]. An increase of the adsorbant led to a negative shift of the point of zero charge. At higher concentrations, a positive *pzc* shift indicates a skew position of the *pT* molecules. This is also true for mixtures with *PEG 400*, where the same *pzc* changes are observed at higher *pT* concentrations. However, in mixtures containing *PEG 10000* and *pT* the *pzc* values shift only towards negative potentials which indicates a flat orientation of the *pT* molecules on the mercury in these solutions. The *pzc* and surface tension values presented in Fig. 3 and Table 1 point at stronger adsorption of *PEG 10000* than for *PEG 400*.

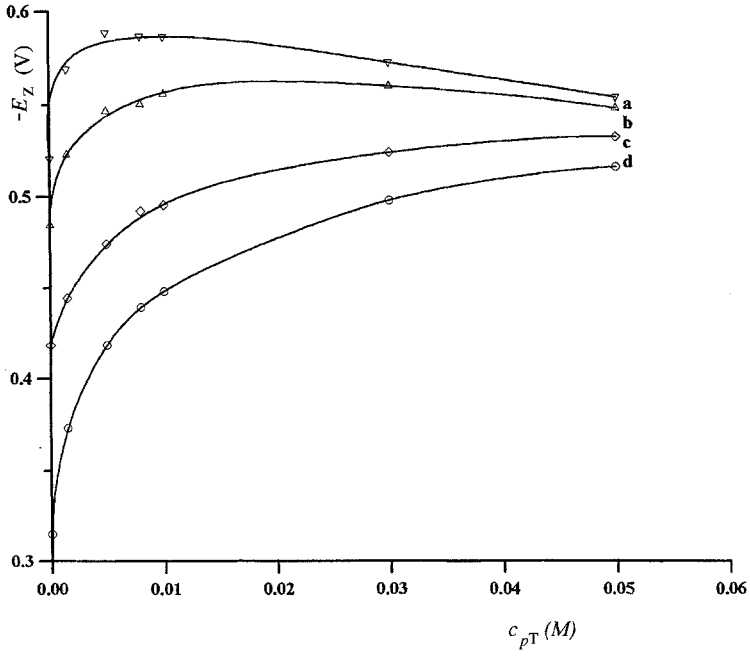

Fig. 3. Potential of zero charge ($-E_z$) *vs.* SCE as a function of the concentration of *pT* in the bulk for a) 1 *M* $NaClO_4 + 10^{-4}$ *M PEG 400*, b) 1 *M* $NaClO_4 + 5 \cdot 10^{-4}$ *M PEG 400*, c) 1 *M* $NaClO_4 + 10^{-4}$ *M PEG 10000*, d) 1 *M* $NaClO_4 + 5 \cdot 10^{-4}$ *M PEG 10000*

Table 1. Surface tension (γ, $mN \cdot m^{-1}$) for E_z of *PEG/pT* mixtures

C_{pT} (M)	$C_{PEG\,400}$ (M)		$C_{PEG\,10000}$ (M)	
	10^{-4}	$5 \cdot 10^{-4}$	10^{-4}	$5 \cdot 10^{-4}$
0	410.1	404.0	382.5	379.4
0.0015	401.1	398.7	381.6	376.6
0.005	396.3	393.6	378.2	374.3
0.008	393.3	390.9	376.6	373.1
0.01	391.8	389.8	375.4	371.9
0.03	383.8	380.8	368.3	366.3
0.05	378.5	374.6	365.4	362.3

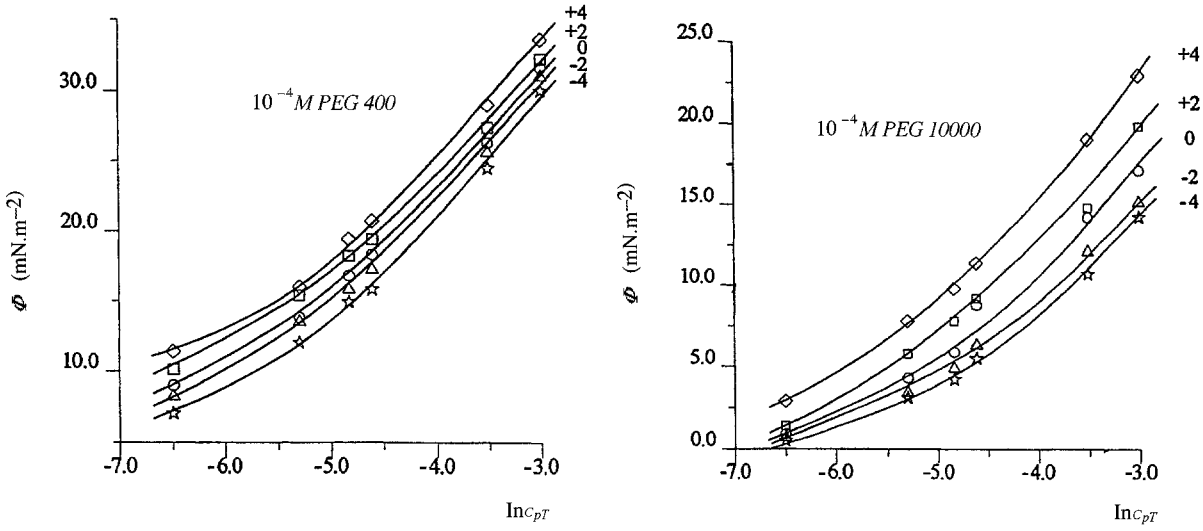

Fig. 4. Surface pressure as a function of pT concentration in the bulk; the electrode charges (σ_M in $10^{-2}\,C \cdot m^{-2}$) are indicated for each curve

The data obtained from the integration of the differential capacity curves were then used to calculate *Parsons'* auxiliary function [15] $\xi = \gamma + \sigma \cdot E$ (γ: surface tension, σ: electrode charge, E: electrode potential) and the surface pressure [16] $\Phi = \Delta\xi = \xi^0 - \xi$ (ξ^0: average value of supporting electrolyte for the determined constant concentration of *PEG* without pT, ξ: the same, but with addition of pT). Fig. 4 shows characteristic plots of Φ *vs.* $\ln c_{pT}$ for selected constant concentrations ($10^{-4}\,M$ *PEG 400* or $10^{-4}\,M$ *PEG 10000*).

According to the *Gibbs* adsorption isotherm, the relative surface excess of pT is given by

$$\Gamma'_{pT} = \frac{1}{RT}\left(\frac{\partial \Phi}{\partial \ln c_{pT}}\right)_{\sigma, c_{PEG}} \tag{1}$$

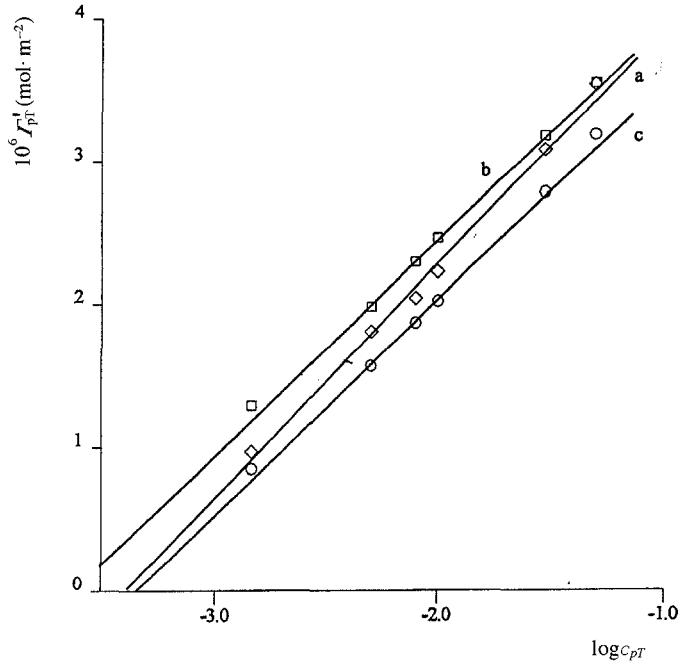

Fig. 5. Relative surface excess of pT as a function of the concentration of pT in the bulk at *pzc* for a) 1 *M* $NaClO_4$, b) 1 *M* $NaClO_4 + 10^{-4}$ *M PEG 400*, c) 1 *M* $NaClO_4 + 10^{-4}$ *PEG* 10000

where c_{pT} is the bulk concentration of pT. The estimated error in these calculations is approximately 10 times that in the capacity data, that is from $\pm 2\%$ to $\pm 5\%$.

The obtained values of Γ'_{pT} indicate that the adsorption of pT both in 1 *M* $NaClO_4$ and in the presence of *PEG 10000* is enhanced at positive electrode charges and diminished at negative ones. In the presence of *PEG 400*, Γ'_{pT} does not depend on the electrode charge. It should be emphasized that the adsorption of pT is decreased in the presence of *PEG 10000* but is increased particularly for $\sigma_M \leqslant 0$ in the presence of *PEG 400*. Such a synergetic character of the pT adsorption in the presence of *PEG 400* was observed also in the *m*-toluidine-*PEG* system. Figure 5 presents the dependence Γ'_{pT} *vs.* pT at *pzc* for solutions containing only pT in 1 *M* $NaClO_4$ (curve a) and for those with the addition of 10^{-4} *M PEG 400* (curve b) or 10^{-4} *M PEG 10000* (curve c). A rectilinear character of this dependence is, undoubtedly, due to low pT concentrations caused by the solubility of pT under the applied conditions.

Adsorption isotherms

The adsorption of pT was further analyzed on the basis of the surface pressure data using the *Frumkin* isotherm. The constants of the *Frumkin* isotherm were determined from Eq. (2), where x is the molar fraction of pT, Θ is the coverage, A is the interaction constant, and β is the adsorption coefficient $\beta = \exp(-\Delta\bar{G}^0/RT)$.

$$\beta x = [\Theta/(1-\Theta)]\exp(-2A\Theta) \tag{2}$$

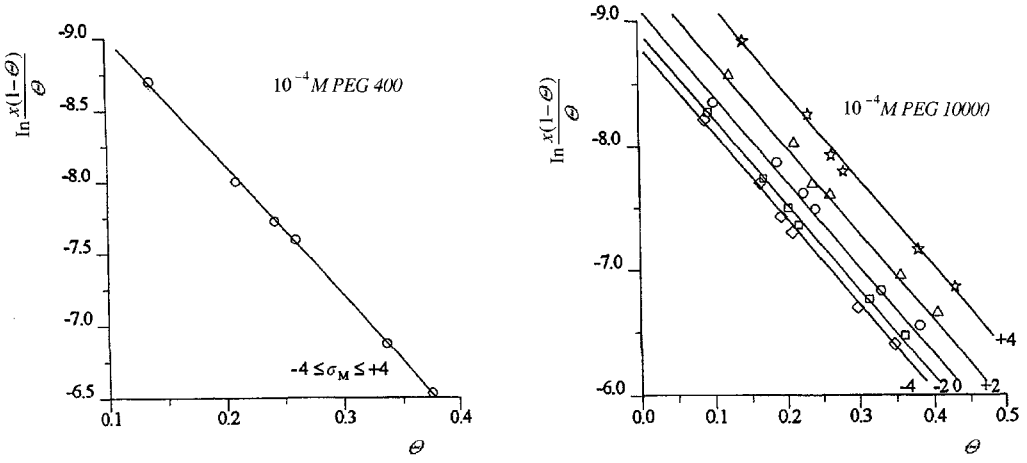

Fig. 6. Linearity test of the *Frumkin* isotherm; the electrode charges (σ_M in 10^{-2} C·m^{-2}) are indicated for each line

The surface excess at saturation Γ_s was estimated by extrapolating ($1/\Gamma'$ *vs.* $1/c_{pT}$ at different charges and different c_{PEG} to $1/c_{pT} = 0$.

The Γ_s values for pT obtained in 10^{-4} *M* and $5 \cdot 10^{-4}$ *M PEG 400* solutions are $9.4 \cdot 10^{-6}$ and $9.1 \cdot 10^{-6}$ mol·m^{-2}, and those in 10^{-4} *M* and $5 \cdot 10^{-4}$ *M PEG 10000* solutions $8.4 \cdot 10^{-6}$ and $7.9 \cdot 10^{-6}$ mol·m^{-2}. Thus, they are always lower than the theoretical value which is $9.7 \cdot 10^{-6}$ mol·m^{-2} for pT [17]. The area occupied by one molecule of pT ($S \equiv 1/\Gamma_s$) increases from the theoretical value of 0.17 nm^2 to a maximum of 0.21 nm^2 obtained in the $5 \cdot 10^{-4}$ *M PEG 10000* solution.

Figure 6 presents a linearity test of the *Frumkin* isotherm for 10^{-4} *M PEG 400* or 10^{-4} *M PEG 10000*. As follows from the figure, the interaction constant A is independent of the electrode charge in both cases and is -4.5 and -3.5 for *PEG 400* and *PEG 10000*, respectively. In the presence of $5 \cdot 10^{-4}$ *M PEG 400* or *PEG 10000*, the values of parameter A are smaller (-3.6 and -3.1, respectively). A slight dependence of parameter A on the charge is found also for pT in 1 *M* $NaClO_4$, *i.e.* for $\sigma_M = -4\,\mu$C·cm^{-2} A amounts to -3.7, and for the other electrode charges it is -3.5. It follows that the increase in concentrations of *PEG 400* and *PEG 10000* is accompanied by a decrease of repulsion among pT molecules which is associated with better ordering of the double layer structure on the electrode surface. The value of the free energy of adsorption $\Delta\bar{G}^0$ was determined from the extrapolation of the linear graphs of the dependence $\ln(x \cdot (1 - \Theta)/\Theta)$ *vs.* Θ to the value $\Theta = 0$. The values of $\Delta\bar{G}^0$ for pT in 1 *M* $NaClO_4$ in the range of electrode charges from -4 to $+4\,\mu$C·cm^{-2} vary from -21.9 kJ·mol^{-1} to -22.6 kJ·mol^{-1}, whereas in the presence of both 10^{-4} *M* and $5 \cdot 10^{-4}$ *M PEG 400* these values do not depend on the charge and amount to -24.6 kJ·mol^{-1} and -23.7 kJ·mol^{-1}, respectively. Figure 7 presents the dependence of $\Delta\bar{G}^0(pT)$ on the charge in the presence of *PEG 10000*. In this case, though only for $\sigma_M > 0$, the values of $\Delta\bar{G}^0$ are greater than those obtained in 1 *M* $NaClO_4$. A linear dependence of $\Delta\bar{G}^0$ on σ_M in Fig. 7 indicates a preferential contribution of a permanent dipole to the free energy of adsorption as in the case of

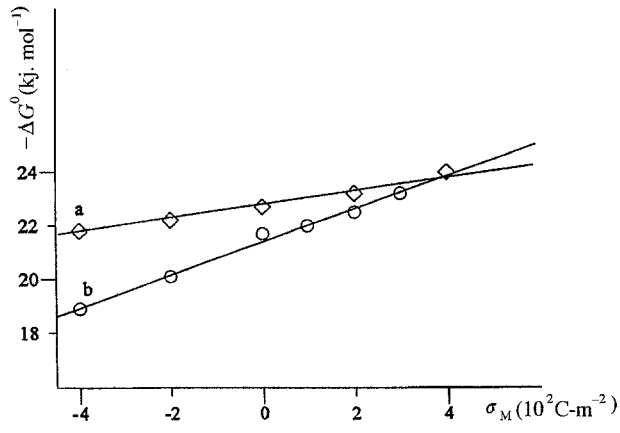

Fig. 7. Variation of the free energy of adsorption due to surface charge density for 10^{-4} *M PEG 10000* (a) and $5 \cdot 10^{-4}$ *M PEG 10000* (b)

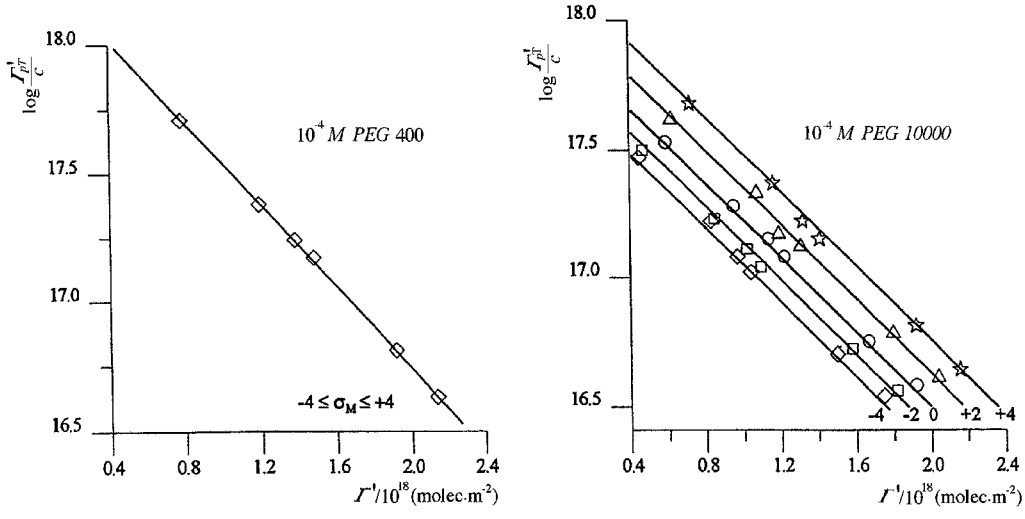

Fig. 8. Linearity test of the virial isotherm; the electrode charges (σ_M in 10^{-2} C·m^{-2}) are indicated for each line

thiourea [16]. As the values of Γ_s obtained for pT in the presence of both *PEG 400* and *PEG 10000* are different from the theoretical ones, the virial isotherm was used for the description of pT adsorption. Figure 8 shows the linearity-test of the virial isotherm, *i.e.* the dependence of $\log(\Gamma'_{pT}/c)$ *vs.* Γ'_{pT} for 10^{-4} *M PEG 400* and *PEG 10000*. The values of the two-dimensional second virial coefficient (B) which encloses corrections for both intermolecular interactions and molecular size in all examined systems are greater than the value of 0.5 nm^2·molec^{-1} obtained for pT in 1 *M* $NaClO_4$. The corresponding values in the presence of 10^{-4} *M* and $5 \cdot 10^{-4}$ *M PEG 400* are 1.6 and 1.4 nm^2·molec^{-1}, respectively, but in the presence of both concentrations of *PEG 10000* they are equal being 0.7 nm^2·molec^{-1}. However, the values of $\Delta\bar{G}^0$ confirm the results obtained from the *Frumkin* isotherm.

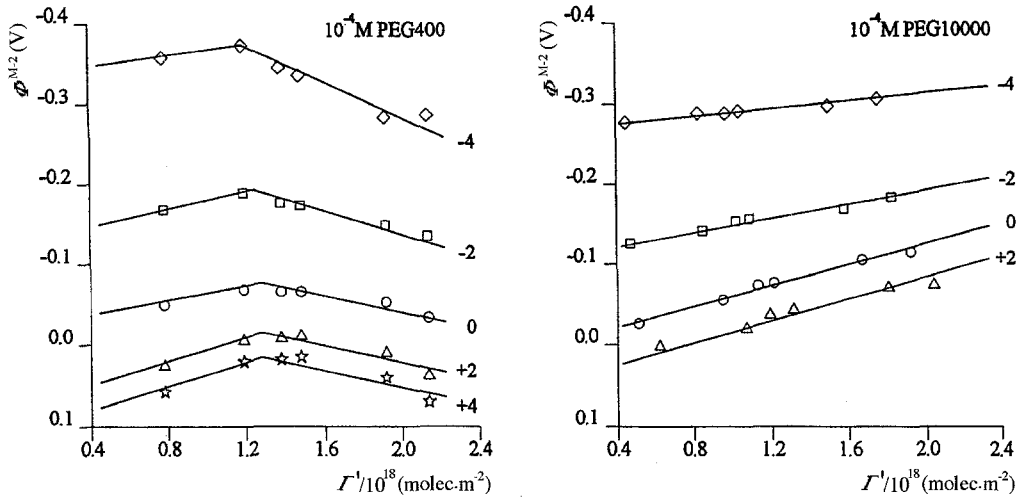

Fig. 9. Potential drop across the inner layer (Φ^{M-2}) as a function of the quantity of pT adsorbed at constant electrode charges (σ_M in 10^{-2} C·m^{-2})

The *Gibbs* surface excess of pT (Γ'_{pT}) was further plotted against the potential drop Φ^{M-2} across the inner layer at constant charges. They are shown in Fig. 9. The potential drop across the diffuse layer was calculated using the *Gouy-Chapman* theory. The potential drop in the inner *Helmholtz* plain (IHP) increases linearly with Γ'_{pT} when *PEG 10000* is present. This confirms the congruency of the obtained isotherms in relation to the electrode charge. With *PEG 400*, however, Φ^{M-2} decreases above a critical Γ'_{pT}. This is suggested to be explainable by partial charge transfer [18] but still has to be demonstrated.

Kinetics of Zn(II) ion reduction

The results presented earlier concerning pT adsorption in the presence of *PEG 400* or *PEG 10000* provide information about the structure of a mixed adsorption layer, but they cover a range of strong adsorption potentials of these substances. Studies on the kinetics of Zn(II) as a pilot ion are expected to broaden this range. The diffusion coefficients, necessary for the determination of the standard rate constant k_s^{app} of Zn(II) reduction, reach a minimum value in solutions containing maximum concentrations of pT ($5.6 \cdot 10^{-6}$ cm^2·s^{-1} and $5.3 \cdot 10^{-6}$ cm^2·s^{-1} for *PEG 400* and *PEG 10000*, respectively). Therefore, the difference between the reversible half-wave potential $E^r_{1/2}$ for Zn(II) and the formal potential E^0_f of Zn(II) reduction in the studied mixtures was -7 mV at maximum. With increasing pT concentration, the values of $E^r_{1/2}$ change from -0.985 V to -0.995 V [7]. In the presence of 5.10^{-4} *M PEG 400* or $5 \cdot 10^{-4}$ *M PEG 10000*, these changes range from -1.003 V to -0.979 V and from -1.085 to -1.025 V, respectively. Figure 10 presents a logarithmic dependence of k_s^{app} of the Zn(II) ion reduction on the pT concentration.

The presented dependences of $\log k_s^{app}$ on $\log c_{pT}$ referring to solutions containing *PEG* (curves b, c, d) are not linear. Similar dependences obtained in systems

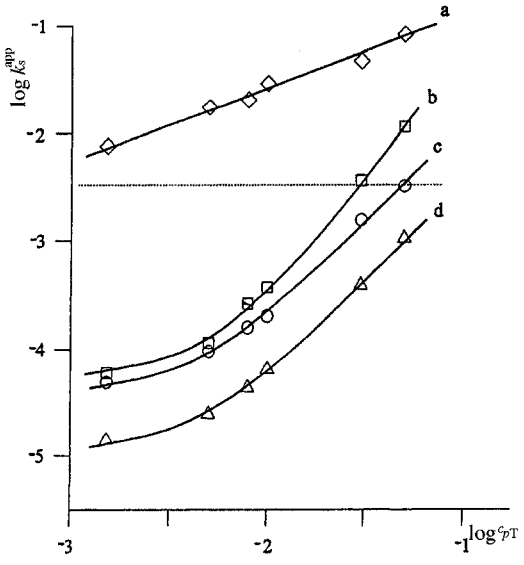

Fig. 10. Plots of $\log k_s^{app}$ for the (Hg)Zn(5·10^{-3} *M*)/Zn(II)(5·10^{-3} *M*) couple *vs.* $\log c_{pT}$ for different contents of *PEG*: a) 0 *M*, b) 10^{-4} *M*, *PEG 400*, c) 5·10^{-4} *M PEG 400*, d) 10^{-4} *M PEG 10000*; the dashed line denotes $k_s = 3.31 \cdot 10^{-3}$ cm·s^{-1} for Zn(II) in 1 *M* $NaClO_4$

studied earlier (*n*-butanol-thiourea [6], *n*-butanol-toluidine [7], and *PEG*-thiourea [8]) were rectilinear.

The kinetics of Zn(II) ions reduction depends on the concentration of *PEG 400*. In the presence of 10^{-4} *M* and 5·10^{-4} *M PEG 400*, the values of k_s^{app} are $3.27 \cdot 10^{-5}$ cm·s^{-1} and $2.63 \cdot 10^{-5}$ cm·s^{-1}, respectively. A similar effect is observed in the presence of *pT*. In the presence of *PEG 10000*, the value k_s^{app} is $6.00 \cdot 10^{-6}$ cm·s^{-1} and does not depend on the concentration which is, undoubtedly, due to a large coverage of the electrode surface with a monolayer which is not very tight. Also, the values k_s^{app} obtained in the *pT* and *PEG 10000* mixtures do not depend on the concentration of the second component. If the values k_s^{app} obtained in the *pT* and *PEG 400* mixtures are comparable with the value k_s^{app} obtained for Zn(II) ions reduction in 1 *M* $NaClO_4$, then compensation of inhibiting and accelerating effects takes place. Such a compensation occurs for the concentration ratio *pT*:*PEG 400* ≈ 300 or 100 when the concentrations of *PEG 400* are 10^{-4} *M* or 5·10^{-4} *M*, respectively. There is evidence for higher ordering of the double layer structure in the presence of *PEG 400* which allows better access of *pT* molecules to the surface. Such a compensation does not occur in the presence of *PEG 10000*, but the concentration ratio *pT*:*PEG 10000* being 870 or 175 for 10^{-4} *M* or 5·10^{-4} *M PEG 10000*, respectively, can be determined from the extrapolation curve d. As for *PEG 400*, this ratio also decreases with the increase of *PEG 10000* concentration. The results show that *pT* and *PEG* coadsorption occurs also at potentials distant from *pzc* and that adsorption of *PEG 10000* is stronger than that of *PEG 400*.

From the slope of the straight line a in Fig. 10 and the curves b, c, and d in the point of compensation, an electrode process acceleration coefficient could be determined ($\Delta \log k_s^{app} / \Delta \log c_{pT}$) which is 0.64 for Zn(II) ions reduction in 1 *M* $NaClO_4$ in the presence of *pT* and increases to 2.44 in the presence of both *PEG 400* and *PEG 10000*. This could explain that the electron transfer process $Zn(II) + 2\bar{e} \rightarrow Zn^0$ is accelerated by the greater *pT* molecule lability induced by the presence of *PEG*.

Experimental

The measurements were carried out with a polarograph PA-4 by Laboratorni Pristroje – Prague and EG & G PARC Instrument models 388 and 270 employing a static mercury drop electrode (SMDE) manufactured by Laboratorni Pristroje–Prague (the hanging drop surface was 0.01781 cm^2). The reference electrode was a saturated calomel electrode with NaCl (SCE) or a Ag/AgCl electrode. A platinum spiral was used as an auxiliary electrode. The reference electrode was connected to the cell *via* a salt bridge filled with cell solution. The potentials are referred to the SCE.

The double layer capacity was measured using the ac impedance technique at a frequency of 800 Hz with a set-up for electrochemical measurements (ATLAS-91, made at the Electronic System Plants Atlas-Sollich in Gdańsk) controlled by a computer. The capacitance was measured with a precision of $\pm 0.2\%$. The reproducibility of the average capacity measurements was $\pm 1\%$. A few measurements [19] were also carried out at 200–1500 Hz in order to check the frequency dependence of the results. In the potential range studied no dispersion of the capacitance was observed. A dropping Hg electrode constructed according to *Randless* [20] was used. The balance of the bridge was achieved after 10 s of the drop growth. The drop time was 12 s, and the Hg flow rate 0.762 $mg \cdot s^{-1}$ at a mercury column height of 50 cm. The *pzc* value was measured for each solution using a streaming mercury electrode with an accuracy ± 0.2 mV. Interfacial tension (γ) at *pzc* was measured by the maximum bubble pressure following the *Schiffrin*'s method [21].

Kinetic data were obtained by impedance measurements (for the *pT-PEG 400* systems) or using the cyclic voltammetric technique (for the *pT-PEG 10000* systems) over a wide range of sweep rates (0.005–5 $V \cdot s^{-1}$). The complex cell impedance was obtained at different frequencies in the range from 100 to 25000 Hz at the formal potential. The formal potentials of the reduction of Zn(II) were obtained from cyclic voltammetry with a reproducibility of ± 0.002 V. The ohmic resistance of the electrolyte solution was obtained as the real impedance component at a frequency of 10000 Hz and at a potential outside the faradaic region.

The approximate diffusion coefficients of Zn(II) in the examined solutions were calculated from limiting currents using the *Ilkovic* equation [22]. The polarographic wave of Zn(II) in 0.1 *M* KNO_3 with a Zn(II) diffusion coefficient of $D = 6.9 \cdot 10^{-6}\ cm^2 \cdot s^{-1}$ [23] was used as a standard. The diffusion coefficient of zinc in mercury which is required for further calculations was taken from the literature [24] as equal to $1.67 \cdot 10^{-5}\ cm^2 \cdot s^{-1}$.

Measurements were carried out in 1 *M* $NaClO_4$ solution of *pH* 3 in a *pT* concentration range from 0.0015 *M* to 0.05 *M* and at two *PEG* concentrations (10^{-4} and $5 \cdot 10^{-4}$ *M*) as well as in their corresponding mixtures at 298 ± 1 K. The solutions were prepared from freshly bidistilled water and analytical grade chemicals (Merck or Fluka). Nitrogen, previously purified using vanadium(II) sulfate solution, served to deoxygenate the electrolyte. Mercury was distilled twice.

Acknowledgements

The author thanks Professor *K. Sykut* for valuable discussions.

References

[1] Nikitas P (1988) J Electroanal Chem **251**: 235
[2] Trasatti S (1986) In: Silva AF (ed) Trends in Interfacial Electrochemistry, p 1
[3] Lipkowski J, Buess-Herman C, Lambert JP, Gierst L (1986) J Electroanal Chem **202**: 169
[4] Sykut K, Saba J, Marczewska B, Dalmata G (1984) J Electroanal Chem **178**: 295
[5] Sykut K, Dalmata G, Marczewska B, Saba J (1991) Pol J Chem **65**: 2241
[6] Saba J (1994) Electrochim Acta **39(5)**: 711
[7] Saba J (1995) Collect Czech Chem Commun **60**: 1457
[8] Saba J (1996) Electrochim Acta **41**: 297

[9] Saba J (1996) Collect Czech Chem Commun **61**: 99
[10] Rösch M (1956) Kolloid Z **147**: 80
[11] Rösch M (1957) Kolloid Z **150**: 153
[12] Damaskin BB (1969) Elektrochimija **5**: 524
[13] Jehring H (1974) Elektrosorptionsanalyse mit der Wechselstrompolarographie. Akademie Verlag, Berlin
[14] Dalmata G, Nieszporek J (1994) Polish J Chem **68**: 2009
[15] Parsons R (1955) Trans Faraday Soc **51**: 1581
[16] Parsons R (1961) Proc Roy Soc A **261**: 79
[17] Joshi KM, Mahajan SJ, Bapat MR (1974) J Electroanal Chem **54**: 371
[18] Ikeda O, Jimbo H, Tamura H (1982) J Electroanal Chem **137**: 127
[19] Baars A, Knapen JWJ, Sluyters-Rehbach M, Sluyters JH (1994) J Electroanal Chem **368**: 293
[20] Randles JEB (1962) Progress in Polarography, vol 1. Wiley Interscience, New York, p 123
[21] Schiffrin DJ (1969) J Electroanal Chem **23**: 168
[22] Ilkovic D (1934) Collect Czech Chem Commun **6**: 498
[23] Turnham DS (1965) J Electroanal Chem **10**: 19
[24] Furman NS, Cooper WCh (1950) J Am Chem Soc **72**: 5667

Received January 10, 1996. Accepted (revised) August 26, 1996